



# ACOUSTIC SOURCE DETECTION FOR MOVING SOUND SOURCES BASED ON THE 2.5D BEM

Christian Kasess and Wolfgang Kreuzer and Prateek Soni and Holger Waubke  
Acoustics Research Institute, Austrian Academy of Sciences  
Dominikanerbastei 16, 1010, Vienna, Austria

## Abstract

The Helmholtz boundary element method (BEM) is a versatile tool to calculate the sound field around scattering structures in 2D and 3D. For infinitely long structures with constant cross-section the 2.5D approach can be used to increase the efficiency of the BEM when solving problems in 3D. Furthermore, the 2.5D setting allows a straightforward treatment of uniformly moving sources when the direction of motion is along the infinite dimension.

In this work, an inverse approach will be presented for the localization of uniformly moving tonal sources. This approach is based on the 2.5D BEM and acts entirely in the frequency domain. It allows for the presence of scattering objects in the sound propagation path and, as it does not require cutting the microphone signal into short, quasi-stationary segments, a high spectral resolution can be achieved. Furthermore, using the BEM also allows for the treatment of different types of sources such as vibrating parts on a moving scattering structure, point or incoherent line sources.

In this work, the general properties of the mapping between source and microphones, that is inverted using a Tikhonov regularization, will be investigated. The feasibility of the 2.5D approach is demonstrated using simulated data.

## 1 INTRODUCTION

Microphone arrays are commonly used for detecting and localizing sound sources. By far the most popular method of choice is beamforming and all its flavors (e.g. [16]).

For moving sources, the typical approach is to use a moving focus either applied purely in the frequency domain [4] or, more commonly, at least partially (e.g.[6, 19]) or fully (e.g.[1]) in the time domain. With the latter methods, the pressure caused by a moving source is formulated in the time domain, thus, the Doppler shift can be taken into account in a relatively straightforward manner. In contrast to the pure frequency domain approach in [4] that is based on “snapshots” of the moving object, no assumptions about small displacements are necessary.

While in conventional beamforming the strength of each source is determined independently, inverse methods solve a joint optimization problem applying some sort of regularization for the typically undetermined system, see e.g. [15, 20]. In addition to the free-field setting, numerical methods such as the boundary element method (BEM) or the finite element method (FEM) allow the inclusion of scattering structures or more complex source models (e.g. [5, 18]).

Recently, an inverse method based on a 2.5D approach for sound source localization of single-frequency sources moving at a constant speed was presented in [13]. Although defined fully in the frequency domain, this approach has the advantage that effects like the Doppler shift can be included in the formulation in closed form. The 2.5D approach is based on the assumption of a constant cross-section in the  $y$ - $z$  plane. In contrast to pure 2D methods, 2.5D methods allow for a varying soundfield along  $x$  which is achieved via a spatial Fourier transform of the Helmholtz equation along  $x$  into the wavenumber domain. An inverse Fourier transform of many 2D calculations for different 2D-wavenumbers is used to get back to the spatial domain in  $x$  (see e.g., [2, 3, 10–12, 14, 17, 21]).

The approach presented in [13] operates fully in the frequency domain and compensates for the spectral leakage of the *discrete* Fourier transform (DFT) which needs to be applied to the measured microphone array data. It was validated using simulated scenarios in the free field and with a reflecting ground present. In the present work, it will be demonstrated that using the 2.5D BEM allows for more complex scenarios including velocity sources and scattering structures. In the following, a brief overview of the general idea of the approach will be given (for details please refer to [13]) and extensions with regard to the source model will be indicated. Simulated data will be used to evaluate the approach.

## 2 METHODS

### 2.1 Uniformly moving sources

As a starting point, a source region containing  $L$  potential moving sources at positions  $\mathbf{x}_{s,\ell} = (x_{s,\ell}(t), y_{s,\ell}, z_{s,\ell})^\top$ ,  $\ell = 1, \dots, L$  and a microphone array with  $N$  microphones at positions  $\mathbf{x}_{r,n} = (x_{r,n}, y_{r,n}, z_{r,n})^\top$ ,  $n = 1, \dots, N$ , and typically  $N < L$  are defined. The argument  $t$  indicates, that the source is moving along  $x$ . For the case of a source moving at a constant speed of  $v_s$ , the  $x$ -position is given as:  $x_{s,\ell}(t) = x_{s,\ell} + v_s t$ . The time-dependent pressure at the  $n$ -th receiver position caused by a uniformly moving point source at the  $\ell$ -th source position is given as (for a derivation see e.g. [2])

$$p_{n\ell}(t) = \frac{1}{(2\pi)^2} \int_{-\infty}^{\infty} \int_{-\infty}^{\infty} \hat{s}_\ell(\omega - v_s k_x) \hat{q}_{n\ell} \left( \sqrt{\omega^2/c^2 - k_x^2} \right) e^{ik_x(x_{r,n} - x_{s,\ell})} e^{-i\omega t} dk_x d\omega. \quad (1)$$

$\hat{s}_\ell(\omega - v_s k_x)$  is the temporal Fourier transform of the source signal  $s_\ell(t)$  evaluated at  $\omega - v_s k_x$ ,  $\hat{q}_{n\ell}(\cdot)$  is the 2D BE solution for the  $\ell$ -th source at the  $n$ -th receiver at the 2D wavenumber  $k_2 = \sqrt{\omega^2/c^2 - k_x^2}$ . Being a 2D solution,  $\hat{q}_{n\ell}(\cdot)$  only depends on the scatterer's cross-section and the source positions in the  $y$ - $z$ -plane and is independent of  $x$ .

Eq. (1), which was used in [13], can immediately be extended to sources modeled by velocity/pressure boundary conditions, however, Eq. (1) implicitly assumes that along  $x$  the sources

are given by  $s(t)\delta(x - v_s t)$ , thus they are point-like, i.e. infinitely short. More general, sources can be point sources (omnidirectional, dipoles but also higher moments) as well as moving pressure or velocity boundary conditions. The latter are defined on one or more boundary elements of the 2D-mesh of the cross-section of the scatterer in the  $y$ - $z$ -plane. Irrespective of the type, sources extending in  $x$  can also be treated in a straightforward manner in the 2.5D framework as long as the spatial Fourier transform of the source strength along  $x$  exists. Details for the stationary case and velocity boundary conditions can be seen in [14], where the radiation of a rail on a railway track is modeled using the 2.5D BEM. Following the derivation for Eq. 1 as given in [2] and defining a more general type of source  $s(t)u(x - v_s t)$  leads to the transfer function from a source at  $\mathbf{x}_{s,\ell}$  to the sound pressure at  $\mathbf{x}_{r,n}$

$$p_{n\ell}(t) = \frac{1}{(2\pi)^2} \int_{-\infty}^{\infty} \int_{-\infty}^{\infty} \hat{s}_\ell(\boldsymbol{\omega} - v_s k_x) \hat{u}_\ell(k_x) \hat{q}_{n\ell} \left( \sqrt{\boldsymbol{\omega}^2/c^2 - k_x^2} \right) e^{ik_x(x_{r,n} - x_{s,\ell})} e^{-i\boldsymbol{\omega}t} dk_x d\boldsymbol{\omega}, \quad (2)$$

which now includes a weighting according to the Fourier transform of the  $x$ -dependency of the source,  $\hat{u}_\ell(k_x)$ .

In a real scenario, the measured sound pressure at the receiver positions is sampled and a discrete Fourier transform (DFT) is used to transform the time signals to the frequency domain. Usually, a time window (e.g. a Hann window) is applied beforehand to reduce the spectral leakage between adjacent frequency bins in the DFT spectrum. In [13] it was shown that the effects caused by this windowed DFT can be included in the 2.5D forward calculation through a convolution with the temporal Fourier transform of the time window  $g$ :

$$\hat{p}_{n\ell}[\boldsymbol{\omega}'_m] = \frac{1}{(2\pi)^2} \int_{-\infty}^{\infty} \int_{-\infty}^{\infty} \hat{s}_\ell(\boldsymbol{\omega} - v_s k_x) \hat{u}_\ell(k_x) \hat{q}_{n\ell} \left( \sqrt{\boldsymbol{\omega}^2/c^2 - k_x^2} \right) \hat{g}(\boldsymbol{\omega}'_m - \boldsymbol{\omega}) e^{ik_x(x_{r,n} - x_{s,\ell})} dk_x d\boldsymbol{\omega}. \quad (3)$$

$\hat{p}_{n\ell}[\boldsymbol{\omega}'_m]$  denotes the DFT of the sampled version of  $p_{n\ell}(t)$  subject to a data window  $g$  evaluated at  $\boldsymbol{\omega}'_m$ . The brackets denote the discrete nature of the frequency representation.

To simplify Eq. (3), a harmonic ansatz for  $\hat{s}_\ell$  is used [5]:

$$s_\ell(t) = \sum_{j=1}^J a_{\ell j} e^{-i\omega_j t}, \quad (4)$$

with frequencies  $\omega_j = 2\pi f_j$  and corresponding constant complex amplitudes  $a_{\ell j}$ . In contrast to the stationary case, where each frequency  $f_j$  can be treated separately, the spectral broadening of the measured data due to the Doppler effect for moving sources may lead to overlapping spectra requiring a joint treatment of the harmonic components. To reduce the computational burden for the data presented in this manuscript, only single-frequency sources will be assumed with frequency  $\omega_0 = 2\pi f_0$  and thus  $\hat{s}_\ell(\boldsymbol{\omega}) = a_\ell 2\pi \delta(\boldsymbol{\omega} - \omega_0)$ . Applying the spectrum to Eq. (3) to

and performing the integral over  $\omega$  leads to

$$\begin{aligned}\hat{p}_{n\ell}[\omega'_m] &= \frac{a_\ell}{2\pi} \int_{-\infty}^{\infty} \hat{u}_\ell(k_x) \hat{q}_{n\ell} \left( \sqrt{(v_s k_x + \omega_0)^2 / c^2 - k_x^2} \right) \hat{g}(\omega'_m - v_s k_x - \omega_0) e^{ik_x(x_{r,n} - x_{s,\ell})} dk_x \\ &:= h_{n\ell}[\omega'_m] a_\ell.\end{aligned}\quad (5)$$

$h_{n\ell}[\omega'_m]$  represents the transfer function from the  $\ell$ -th single-frequency source to the  $n$ -th receiver evaluated at a discrete frequency  $\omega'_m = 2\pi f'_m$ . Note that this expression is different from [13] where the  $k_x$ -integral was evaluated. The change was done here as the remaining  $k_x$ -integral is more closely related to the standard formulation of the 2.5D method as used in [2, 12].

## 2.2 Source localization

The details about the inversion procedure are provided in [13]. Briefly, the transfer functions  $h_{n\ell}$  are evaluated at specific frequencies  $\omega'_m$  to be chosen beforehand. The choice of these frequencies is a critical parameter for the method. It was shown that a random selection of  $M > 1$  different frequencies per microphone out of a defined spectral range  $[\omega_-, \omega_+]$  leads to good localization performance. Thus, for each of the  $N$  microphones a different set of frequencies is used. The spectral range to choose from depends mainly on the Doppler effect and thus on the source speed. Defining a set  $\Omega_n$  of  $M$  random frequencies per microphone, the  $L_2$ -regularized inversion can be written as:

$$\min_{\mathbf{a} \in \mathbb{C}^L} \sum_{n=1}^N \left\| \tilde{\mathbf{p}}_n[\Omega_n] - \sum_{\ell=1}^L a_\ell \mathbf{h}_{n\ell}[\Omega_n] \right\|_2^2 + \lambda \sum_{\ell=1}^L |a_\ell|^2, \quad (6)$$

where  $\mathbf{a} = (a_1, \dots, a_L)^\top$  is the source weight vector and  $\tilde{\mathbf{p}}_n[\Omega_n]$  is a vector of dimension  $M$  containing data of the  $n$ -th microphone according to the frequencies defined in the respective set  $\Omega_n$ . Similarly,  $\mathbf{h}_{n\ell}$  is a vector of transfer functions  $h_{n\ell}$  evaluated at the frequencies contained in  $\Omega_n$ . In practice, the vectors  $\mathbf{h}_{n\ell}$  for all  $n$  and  $\ell$  are combined into a single transfer matrix  $\mathbf{H}$  of dimension  $(N \cdot M) \times L$ . The  $L_2$ -regularization (also known as Tikhonov regularization) was used to illustrate the potential resolution that can be achieved without resorting to sparse approaches or deconvolution methods. The regularization factor  $\lambda$  is determined via an L-curve approach [9] as implemented in the MATLAB library *Regularization Tools* [8].

## 3 RESULTS

To evaluate the inverse BEM approach, a scenario including a source object  $O_1$  and a barrier-like object  $O_2$  were defined (blue lines in Fig. 1). Here, no half plane was included allowing for diffraction around the top and the bottom of  $O_2$ . However, including a reflective ground to model, e.g., the efficiency of noise barriers, is straightforward. A microphone array (black dots) was placed 4 m away from the source plane. 63 receiver positions were arranged on a square of 1 by 1 m in an irregular pattern using a Halton sequence [7]. The potential source region for the localization task was defined using a rectangular planar mesh extending 4 m in  $x$  and 1 m in the  $z$ -direction and comprised  $40 \times 20$  elements of dimension  $0.1 \text{ m} \times 0.05 \text{ m}$ . Note that

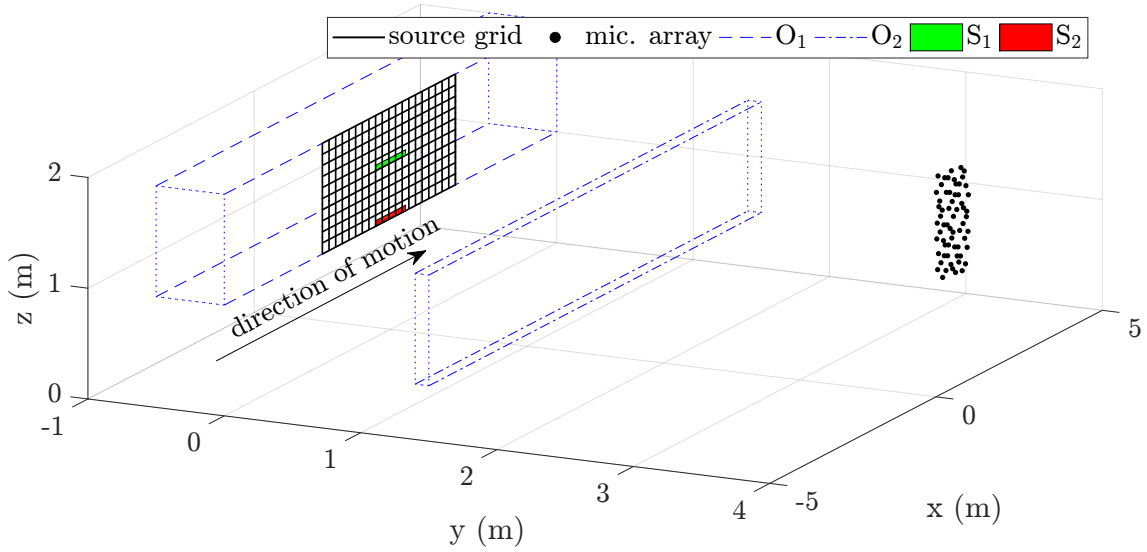


Figure 1: Simulation setting. Blue lines show the outlines of the infinitely long structures  $O_1$  (dashed) and  $O_2$  (dash-dotted). The black lines show the source grid used for the localization located on  $O_1$ . Note that for clarity only groups of four surface elements are shown. The sources for the simulated data are also located on  $O_1$  and delineated by a green ( $S_1$ ) and a red ( $S_2$ ) rectangle. Black dots show the microphone positions.

in Fig. 1 only every other element is shown to avoid cluttering. The source plane is assumed to move with a velocity  $v_g = 50$  m/s in the  $x$  direction and the sources are defined to have a frequency of  $f_0 = 1$  kHz. Please note, that the assumption of a source plane was made to reduce the computational effort. The 2.5D BEM approach would also allow for sources with different  $y$  positions covering, e.g., the full circumference of  $O_1$ . Two moving source regions  $S_1$  and  $S_2$  on the object  $O_1$  were used as indicated by the colored filled rectangular regions within the source grid. The length of the sources was set to 0.9 m centered around  $x = 0$  m. The intensity was set equal along the whole length. Two signals were generated for each source position comprising either  $O_1$  only or  $O_1$  and  $O_2$ . Furthermore, these two scenarios were used to calculate two transfer matrices from the source region to the array:  $O_1$  only or  $O_1$  and  $O_2$ . This led to three meaningful test conditions: two matched conditions, i.e. artificially generated microphone signal and the transfer matrix both are defined with  $O_1$  only (case 1) or  $O_1$  and  $O_2$  (case 2), and a mismatched condition, i.e. the measurement signal was generated with  $O_1$  and  $O_2$  present but the transfer matrix calculated for the case where only  $O_1$  is present was used (case 3). The remaining case with a barrier considered in the transfer matrix but not in the signal generation was not considered as it does not seem to be meaningful in practice. A Hann window of length  $T_g = 1$  s was used in the analysis.

Fig. 2 shows the results for the inversion for all tested conditions. In the left column the higher source position  $S_1$  was used. As can be seen, in the matched conditions the inversion leads to results that closely resemble the true source up to a the blurring due to the use of an  $L_2$ -regularization and a tendency to a slightly elevated source position in case 2. In the mismatched condition, clearly the source map does not identify the true source region but two regions are identified with the stronger region being clearly displaced vertically. Similarly, for the lower

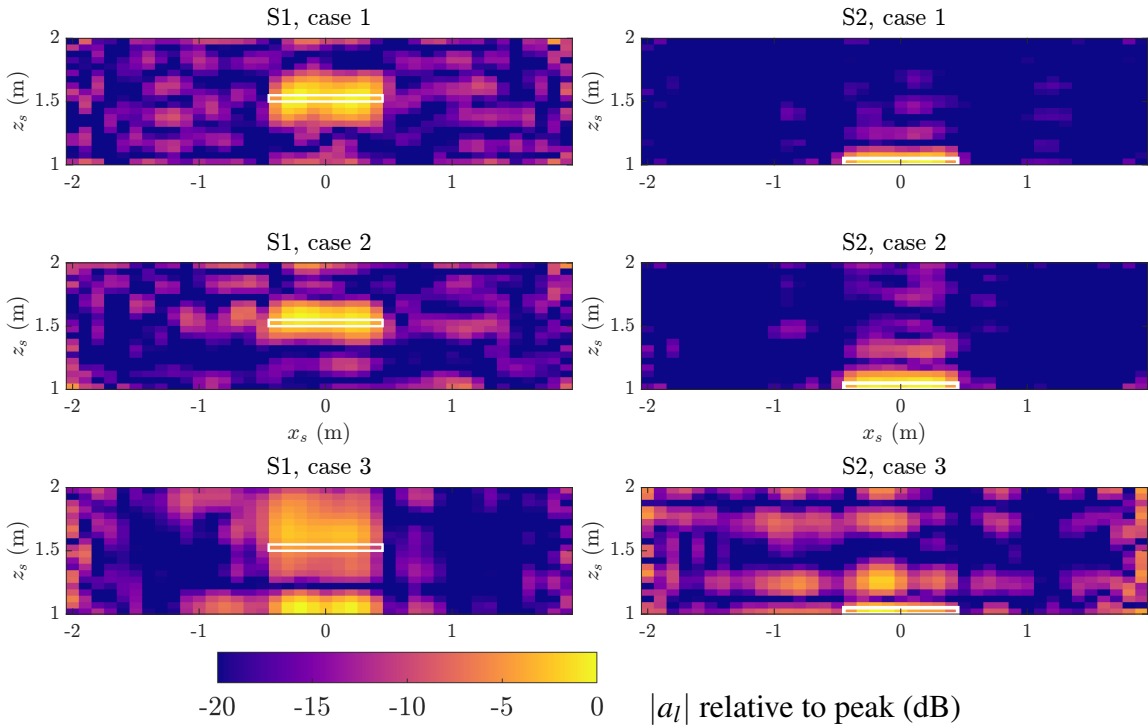


Figure 2: Localization results. Panels show the results of the inversion for different settings. Columns denote different source positions as indicated by the white rectangles. The upper row shows the case where only  $O_1$  was present, in the middle row  $O_1$  and  $O_2$  were present and included in the calculation of the transfer matrix. The lower row shows the case when  $O_1$  and  $O_2$  were used to generate the data, but only  $O_1$  was used in the transfer matrix. The dynamic range was set to 20 dB and the peak was normalized to 0 dB.

source position ( $S_2$ , red rectangle in Fig. 1) the matched condition leads to a good agreement between the true position and the source map whereas the mismatched condition does not yield a satisfying result.

## 4 SUMMARY

Recently a method using a 2.5D approach was developed and validated on moving point sources [13]. In this work, the approach was applied to situations where the 2.5D boundary element method is required. As shown, the inverse 2.5D BEM has a high potential for moving source localization in a complex acoustic setting, enabling the localization of sources which may be shielded. The results of the mismatched condition for signal and transfer matrix also indicate the importance of including scattering structures in the forward problem.

Clearly, there are currently many restrictions. First, using only a single-frequency setting is not very realistic and the extension to more complex stimuli where the harmonic components result in overlapping bands is a matter of current and future work. In order for this extension to be feasible, the efficiency of this computationally costly method is also of major concern.

Furthermore, the inclusion of deconvolution approaches and the use of sparsness-enforcing regularization will be considered in the future.

## 5 ACKNOWLEDGEMENTS

This work was supported by the Austrian Science Fund (FWF) via the DACH project LION (Localization and Identification of moving noise sources, I 4299-N32). The authors would like to thank Nicki Holighaus for providing the programming code for the Halton sequence.

## REFERENCES

- [1] R. Cousson, Q. Leclère, M. A. Pallas, and M. Bérengier. “A time domain CLEAN approach for the identification of acoustic moving sources.” *J. Sound Vib.*, 443(March), 47–62, 2019. ISSN 10958568. doi:10.1016/j.jsv.2018.11.026.
- [2] D. Duhamel. “Efficient calculation of the three-dimensional sound pressure field around a noise barrier.” *J. Sound Vib.*, 197(5), 547–571, 1996.
- [3] J. Fakhraei, R. Arcos, T. Pàmies, and J. Romeu. “2.5D singular boundary method for exterior acoustic radiation and scattering problems.” *Eng. Anal. Bound. Elem.*, 143(June), 293–304, 2022. ISSN 09557997. doi:10.1016/j.enganabound.2022.06.017.
- [4] V. Fleury and J. Bulté. “Extension of deconvolution algorithms for the mapping of moving acoustic sources.” *J. Acoust. Soc. Am.*, 129(3), 1417–1428, 2011. ISSN 0001-4966. doi:10.1121/1.3531939.
- [5] S. Gombots, J. Nowak, and M. Kaltenbacher. “Sound source localization – state of the art and new inverse scheme.” *Elektrotechnik und Informationstechnik*, 138(3), 229–243, 2021. ISSN 0932383X. doi:10.1007/s00502-021-00881-6.
- [6] S. Guerin and C. Weckmüller. “Frequency-domain reconstruction of the point-spread function for moving sources.” In *Proceedings on CD of the 2nd Berlin Beamforming Conference (BeBeC)*, pages CD-ROM. 2008. ISBN 978-3-00-023849-9.
- [7] J. Halton. “On the efficiency of certain quasi-random sequences of points in evaluating multi-dimensional integrals.” *Numerische Mathematik*, 2, 84–90, 1960. ISSN 0888-3270. doi:https://doi.org/10.1007/BF01386213.
- [8] P. C. Hansen. “Regularization Tools Version 4.0 for Matlab 7.3.” *Numerical Algorithms*, pages 189–194, 2007.
- [9] P. C. Hansen and D. P. O’Leary. “The Use of the L-Curve in the Regularization of Discrete Ill-Posed Problems.” *SIAM J. Sci. Comput.*, 14(6), 1487–1503, 1993. ISSN 1064-8275. doi:10.1137/0914086.
- [10] M. Hornikx and J. Forssén. “The 2.5-dimensional equivalent sources method for directly exposed and shielded urban canyons.” *J. Acoust. Soc. Am.*, 122(5), 2532, 2007. ISSN 00014966. doi:10.1121/1.2783197.

- [11] M. Kamrath, P. Jean, J. Maillard, J. Picaut, and C. Langrenne. “Extending standard urban outdoor noise propagation models to complex geometries.” *J. Acoust. Soc. Am.*, 143(4), 2066–2075, 2018. ISSN 0001-4966. doi:10.1121/1.5027826.
- [12] C. Kasess, W. Kreuzer, and H. Waubke. “An efficient quadrature for 2.5D boundary element calculations.” *J. Sound Vib.*, 382, 213–226, 2016.
- [13] C. H. Kasess, W. Kreuzer, P. Soni, and H. Waubke. “Localizing uniformly moving mono-frequent sources using an inverse 2.5D approach.” *preprint, arXiv, submitted to J. Sound Vib.*, 2024. doi:https://doi.org/10.48550/arXiv.2401.16819.
- [14] H. Li, D. Thompson, G. Squicciarini, X. Liu, M. Rissmann, F. D. Denia, and J. Giner-Navarro. “Using a 2.5D boundary element model to predict the sound distribution on train external surfaces due to rolling noise.” *J. Sound Vib.*, 486, 1–37, 2020. ISSN 10958568. doi:10.1016/j.jsv.2020.115599.
- [15] F. Meng, Y. Li, B. Masiero, and M. Vorländer. “Signal reconstruction of fast moving sound sources using compressive beamforming.” *Appl. Acoust.*, 150, 236–245, 2019. ISSN 1872910X. doi:10.1016/j.apacoust.2019.02.012.
- [16] R. Merino-Martínez, P. Sijtsma, M. Snellen, T. Ahlefeldt, J. Antoni, C. J. Bahr, D. Blacodon, D. Ernst, A. Finez, S. Funke, T. F. Geyer, S. Haxter, G. Herold, X. Huang, W. M. Humphreys, Q. Leclère, A. Malgoezar, U. Michel, T. Padois, A. Pereira, C. Picard, E. Sarradj, H. Siller, D. G. Simons, and C. Spehr. “A review of acoustic imaging methods using phased microphone arrays.” *CEAS Aeronaut. J.*, 10, 197–230, 2019. ISSN 18695590. doi:10.1007/s13272-019-00383-4.
- [17] J. Pizarro-Ruiz, E. P. García, and R. Gallego. “Hypersingular boundary integral equation for harmonic acoustic problems in 2.5D domains with moving sources.” *Eur. J. Comput. Mech.*, 28(1-2), 81–96, 2019. ISSN 19585829. doi:10.13052/ejcm1958-5829.28124.
- [18] A. Schuhmacher, J. Hald, K. B. Rasmussen, and P. C. Hansen. “Sound source reconstruction using inverse boundary element calculations.” *J. Acoust. Soc. Am.*, 113(1), 114–127, 2003. ISSN 0001-4966. doi:10.1121/1.1529668.
- [19] T. Schumacher and H. Siller. “Hybrid approach for deconvoluting tonal noise of moving sources.” In *Proceedings on CD of the 9th Berlin Beamforming Conference (BeBeC)*, pages CD–ROM. 2022.
- [20] T. Suzuki. “L1 generalized inverse beam-forming algorithm resolving coherent/incoherent, distributed and multipole sources.” *J. Sound Vib.*, 330(24), 5835–5851, 2011. ISSN 0022-460X. doi:https://doi.org/10.1016/j.jsv.2011.05.021.
- [21] X. Wei and W. Luo. “2.5D singular boundary method for acoustic wave propagation.” *Appl. Math. Lett.*, 112, 106760, 2021. ISSN 18735452. doi:10.1016/j.aml.2020.106760.